Mixing effects in a ternary Hf-Zr-Ni metallic melt

B. Nowak,[1,*] D. Holland-Moritz,[1] F. Yang,[1] Z. Evenson,[2] and A. Meyer[1]
[1]*Institut für Materialphysik im Weltraum, Deutsches Zentrum für Luft- und Raumfahrt (DLR), 51170 Köln, Germany*
[2]*Heinz Maier-Leibnitz Zentrum (MLZ) and Physik Department, Technische Universität München, 85748 Garching, Germany*

(Received 23 October 2017; revised manuscript received 2 February 2018; published 8 March 2018)

We study the effect of the substitution of Zr by Hf on the dynamical behavior in the $Zr_{36}Ni_{64}$ melt. A reduced measured self-diffusion coefficient and a higher measured melt viscosity for an increased amount of Hf were observed. The ternary $Hf_{10}Zr_{25}Ni_{65}$ melt, which exhibits a pronounced deviation from Arrhenius behavior over a studied temperature range of 550 K, can be accurately described by the scaling law of mode-coupling theory (MCT) with almost equal parameters for the self-diffusion and the viscosity. Although we only substitute alloy components with a nearly equal atomic size and the measured overall packing fraction remains almost unchanged, the dynamics in $Hf_{10}Zr_{25}Ni_{65}$ are slower compared to $Zr_{36}Ni_{64}$. This corresponds also to a higher critical temperature T_c and might be induced by different chemical interactions in the melts. The increased T_c results in a significantly smaller difference between liquidus and critical temperature $\Delta T_{LC} = T_L - T_c$ for the ternary melt in comparison with $Zr_{36}Ni_{64}$, which may favor the glass formation in the $Hf_{10}Zr_{25}Ni_{65}$ melt.

DOI: 10.1103/PhysRevB.97.094202

I. INTRODUCTION

Glass-forming metallic liquids are from both technological and scientific points of view attractive for materials science [1]. In order to investigate and understand glass formation on the atomic scale during solidification from the liquid, the interplay between packing fraction, chemical order and atomic dynamics in metallic melts is of fundamental interest [2–7]. An increased packing fraction, which is usually calculated by assuming an ideal hard-sphere mixture with covalent radii as the relevant atomic size, is able to explain, for instance, the more sluggish diffusion in binary Zr-Cu melts towards Cu-rich compositions [8] as well as in Ni-Nb and Ni-Nb-Sn melts towards lower temperatures [9]. In contrast, in Zr-Co-Al and Zr-Ni-Al metallic melts, the dynamical behavior cannot be explained in terms of such a packing fraction argument. Specifically, the addition of Al slows down the transition metal self-diffusion, while actually resulting in a smaller packing fraction compared to that of the corresponding binary melts Zr-Co and Zr-Ni [10]. Apparently, in the case of Al addition, chemical interactions between larger Al atoms and the transition metals strongly influence the atomic dynamics in addition to the impact of the packing fraction. Since all atomic species in Zr-Co-Al and Zr-Ni-Al have a different atomic size, a systematic understanding of the influence of the chemical order becomes much more complicated.

For this reason, we recently investigated the binary melts $Zr_{36}Ni_{64}$ and $Hf_{35}Ni_{65}$, which exhibit a nearly identical packing fraction [11]. The local chemical order in these melts is, however, considerably different, resulting in a markedly different dynamical behavior as probed by quasielastic neutron scattering (QENS). Specifically, we found the activation energy for self-diffusion to be almost twice as large for the $Hf_{35}Ni_{65}$ melt as for $Zr_{36}Ni_{64}$, which could be explained by a smaller interatomic distance between Hf-Hf pairs in comparison to Zr-Zr pairs in these alloy melts [11]. We thus interpreted this effect as a locally denser packing of Hf atoms in $Hf_{35}Ni_{65}$ compared to Zr atoms in $Zr_{36}Ni_{64}$, keeping in mind that the atomic sizes of Zr and Hf should be nearly identical in their pure elemental states [12].

This leads to the question as to what extent the dynamical behavior of the melt is influenced by alloying effects if the overall packing fraction remains constant. This question is particulary relevant for metallic glass formation, as the glass-forming ability (GFA) seems to be generally enhanced by an increased number of different atomic components [2,13].

To study this effect in detail, we have chosen the two binary metallic melts, $Zr_{36}Ni_{64}$ and $Hf_{35}Ni_{65}$, gradually substituted the early transition metal component Zr with Hf, and investigated both the atomic dynamics of the resulting ternary $Hf_{10}Zr_{25}Ni_{65}$ melt by measuring the self-diffusion coefficients using QENS and the macroscopic collective dynamics through measurements of the melt viscosity. The binary systems $Hf_{35}Ni_{65}$ and $Zr_{36}Ni_{64}$ show a dynamical decoupling of self-diffusion coefficients in that the smaller Ni atoms diffuse faster through the melt as compared to larger Hf or Zr atoms. Here, the resulting question is whether such a dynamical decoupling can also be identified in ternary $Hf_{10}Zr_{25}Ni_{65}$ melts and, if so, to what extent it is comparable to that observed in the binary systems. The decoupling between larger and smaller atomic components is, for example, much more pronounced for the multicomponent bulk glass-forming alloy $Zr_{46.75}Ti_{8.25}Cu_{7.5}Ni_{10}Be_{27.5}$ in comparison to the binary systems $Hf_{35}Ni_{65}$ and $Zr_{36}Ni_{64}$ [11,14–16].

The advantage of investigating binary/ternary Hf-/Zr-Ni melts is that we are able to analyze the impact of addition of alloy components on the dynamical behavior at nearly constant packing fraction, consequently reducing the number of different physical parameters under consideration. To do

*benedikt.nowak@dlr.de

so, we substitute only small amounts of melt components with nearly an identical atomic size but having different chemical interactions with the smaller Ni atoms, as evidenced by the different chemical short-range order (CSRO) present in the constituent binary systems [11]. This is an important aspect, as the systematic study of atomic dynamics in multicomponent melts is complicated due to a large number of different atomic interactions as well as different packing fractions between various glass-forming systems.

In the following, we compare the self-diffusion coefficients D and the melt viscosities η for liquid $Hf_{10}Zr_{25}Ni_{65}$ with those in the binary $Hf_{35}Ni_{65}$ and $Zr_{36}Ni_{64}$ melts. We then study the relation between collective and microscopic dynamics, as described by self-diffusion coefficients, for the ternary melt in a temperature range of some 500 K in detail. This connection is viewed in the framework of mode-coupling theory (MCT), which predicts a common scaling law $[(T - T_c)/T_c]^{\gamma}$ for D and η^{-1} with an identical exponent γ when approaching the critical temperature T_c, since both properties are based on the same process in MCT [17]. In addition, identical exponents γ, respectively, a constant product $D \cdot \eta$ as a function of temperature implies the nonvalidity of the Stokes-Einstein (SE) relation [18], which has been previously experimentally verified for $Zr_{64}Ni_{36}$ [19] and $Zr_{46.5}Ti_{18.2}Cu_{7.5}Ni_{10}Be_{27.5}$ [20].

II. EXPERIMENTAL DETAILS

We measured the self-diffusion coefficients for liquid $Hf_{10}Zr_{25}Ni_{65}$ over a temperature range of 550 K using QENS at the time-of-flight spectrometer TOFTOF at the research neutron source Heinz Meier-Leibniz (FRM II) [21,22]. An incoming neutron wavelength of $\lambda_i = 5.1$ Å and a chopper speed of 12 000 rpm result in an instrumental energy resolution of roughly 100 μeV and an accessible q range of 0.25–2.25 $Å^{-1}$ at zero energy transfer. Due to the large absorption cross section of Hf (295 barn at 5.1 Å incident neutron wavelength λ_i) [23] and the high reactivity of Zr- and Hf-based melts, all samples were measured using the containerless processing techniques of electrostatic levitation (ESL) [24] and electromagnetic levitation (EML) [25]. The measurements at high temperatures around 1600 up to 1900 K were performed using EML, because the He atmosphere in the sample chamber reduces the effect of evaporation of sample material. The temperature range below 1600 K was investigated using ESL, since the undercoolability of the samples is enhanced due to processing under high vacuum conditions (pressure$<10^{-6}$ mbar) [24]. Since the relative mass loss during the measurement due to evaporation is smaller than 0.7% (EML), respectively, smaller than 0.1% (ESL), the composition change is $\leqslant 1\%$ and hence effects on the atomic dynamics can be neglected. Due to the lack of a sample container, a high signal-to-background ratio for both techniques is achieved, with a slightly higher ratio for ESL compared to EML. Thus, we are able to perform high-quality measurements even on the strongly absorbing Hf-based samples. The sample sizes were roughly 4 mm (ESL) and 6 mm (EML) in diameter, and the sample temperature was measured using a one-color pyrometer with an absolute accuracy of $\pm$10K [24]. The ESL measurements at 1355, 1400, 1470, and 1550 K represent investigations of the stable as well as the undercooled liquid state, with a liquidus temperature $T_L = 1404$ K. For the EML measurements at 1590, 1675, 1750, and 1905 K a different wavelength of $\lambda_i = 7.0$ Å and chopper speed of 6000 rpm was used, which results in an instrumental energy resolution of roughly 75 μeV and an accessible q range of 0.3–1.8 $Å^{-1}$. The data were treated by subtracting the background from the empty levitation chamber, normalizing to a vanadium standard and correcting for the sample self-absorption. Detailed descriptions of the experimental setup and the data treatment procedure can be found in Refs. [26] and [27], respectively. As a result, we obtain the dynamic structure factor $S(q,\omega)$ and the corresponding intermediate scattering function $S(q,t)$ via Fourier transformation.

The incoherent scattering cross section σ_{inc} of Ni and Hf is 5.2 and 2.6 barn, respectively, resulting in a total incoherent scattering signal from $Hf_{35}Ni_{65}$ that is dominated by contributions from Ni of $\approx$80%. Thus, we determined an average value of the self-diffusion coefficient of Ni and Hf, weighted predominantly by the Ni contribution [11]. Since $\sigma_{\text{inc}}^{\text{Zr}} = 0.02$ barn [23], the incoherent scattering contribution from Zr can generally be neglected. The measured self-diffusion coefficient of $Hf_{10}Zr_{25}Ni_{65}$ is therefore dominated by $\approx$93% Ni contributions.

The melt viscosities for $Hf_{35}Ni_{65}$ and $Hf_{10}Zr_{25}Ni_{65}$ were measured using the oscillating drop technique in ESL. A detailed description of the experimental method in order to calculate the viscosity can be found in Ref. [28]. Density measurements of the $Hf_{10}Zr_{25}Ni_{65}$ melt were also carried out using ESL as described in Ref. [29] to determine the packing fraction.

III. RESULTS

The normalized intermediate scattering functions $S(q,t)/S(q,t=0)$ for $Hf_{10}Zr_{25}Ni_{65}$ are shown in Fig. 1 at $T = 1550$ K for different q values (upper panel) and for $q = 1.25$ $Å^{-1}$ at eight different temperatures (lower panel). As shown in the figure, the combination of QENS and the containerless processing technique leads to high data quality and small statistical errors in the measured intermediate scattering functions. The $S(q,t)$ can be accurately described, as demonstrated in the past for many different glass-forming metallic melts [30–33], by the phenomenological Kohlrausch-Williams-Watts, or stretched exponential, function [34,35]

$$S(q,t) = f_q \exp\{-[t/\langle\tau_q\rangle]^{\beta_q}\}. \quad (1)$$

In this equation, f_q is the Debye-Waller factor, $\langle\tau_q\rangle$ is the mean relaxation time, and β_q is the stretching exponent. In order to determine the stretching exponent β_q and analyze the temperature-dependent line shape of $S(q,t)$, we used the time-temperature scaling [36]. For this purpose, we determined at first f_q and $\langle\tau_q\rangle$ by fitting the intermediate scattering functions $S(q,t)$ in Fig. 1 with a fixed parameter β_q in equation (1). Then, we calculated the master curve by rescaling t and $S(q,t)$ with the relaxation time $\langle\tau_q\rangle$ and the amplitude f_q obtained in the first fitting at each respective temperature. We are thus able to analyze the decay of $S(q,t)$ in a normalized t range of more than two orders of magnitude. By fitting the master curve with β_q as a free parameter in equation

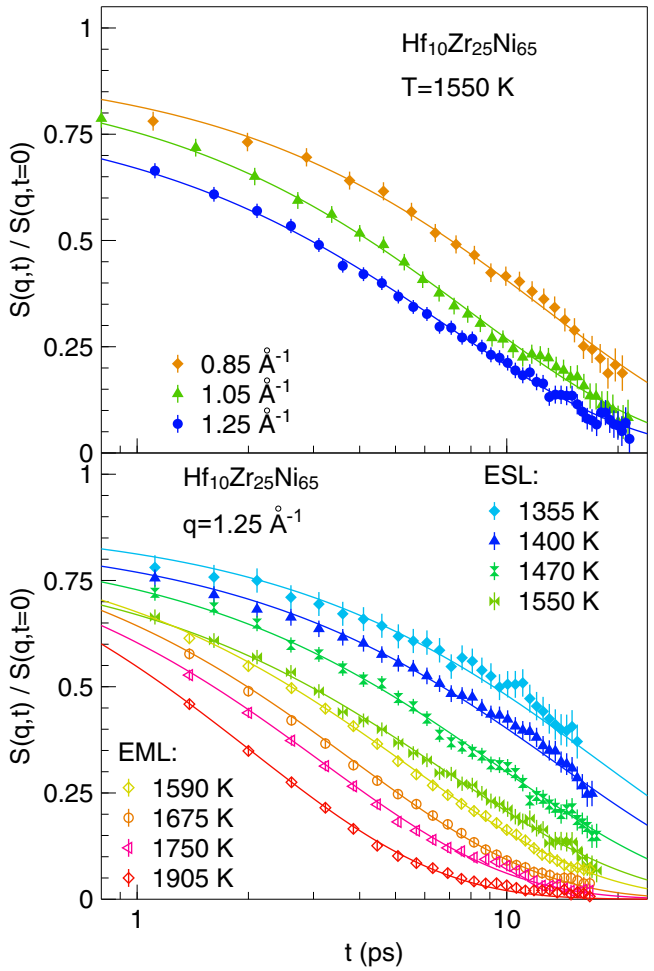

FIG. 1. Upper panel: Normalized intermediate scattering functions for $Hf_{10}Zr_{25}Ni_{65}$ at 1550 K and $q = 0.85$ Å^{-1}, $q = 1.05$ Å^{-1}, and $q = 1.25$ Å^{-1}. The solid lines represent the stretched exponential fit by formula (1). Lower panel: Normalized intermediate scattering function at 1355, 1400, 1470, 1550, 1590, 1675, 1750, and 1905 K for $q = 1.25$ Å^{-1}.

(1), we obtained a stretching exponent of $\beta_q \approx 0.85$. Repeating this procedure in an interative manner using $\beta_q = 0.85$ as a fixed parameter in the fits of $S(q,t)$ and calculating and fitting the master curve again, results in no further significant change of β_q. The result is shown in Fig. 2. As illustrated in the figure, no systematic temperature dependence for β_q can be found, since all temperatures can be well described by using a constant stretching exponent $\overline{\beta_q} = 0.85$ in equation (1) even at the highest measured temperature. The measured $S(q,t)$ in Fig. 1 can be described accurately with $\overline{\beta_q} = 0.85$ in the relevant q range between $q = 0.85$ Å^{-1} and $q = 1.25$ Å^{-1} as well.

This q range is dominated by incoherent scattering and hence, $\overline{\beta_q} = 0.85$ is then further used for determining the relaxation time $\langle\tau_q\rangle$ and the self-diffusion coefficient D. The inverse relaxation time $1/\langle\tau_q\rangle$ is plotted as a function of q^2 in Fig. 3. The self-diffusion coefficients were determined by a linear fit using the relation $D = 1/(\langle\tau_q\rangle q^2)$ between $q^2 = 0.56$ Å^{-2} and $q^2 = 1.69$ Å^{-2} and also containing the origin

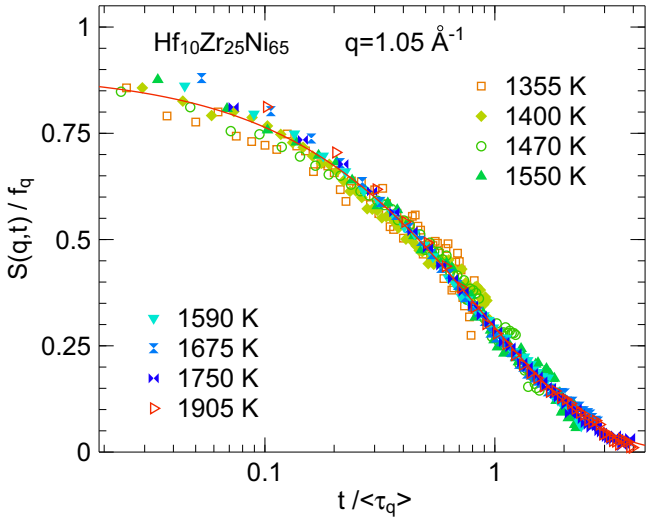

FIG. 2. Time-temperature scaling (master curve) at $q = 1.05$ Å^{-1} for $Hf_{10}Zr_{25}Ni_{65}$. $S(q,t)$ and the time t have been normalized by the calculated f_q, respectively, $\langle\tau_q\rangle$ from the fit with equation (1).

(0,0), since the aforementioned relation is only valid in the hydrodynamic limit $q \to 0$ [37].

The determined self-diffusion coefficients represent a mean value from the analysis in both time and energy transfer domains, i.e., the self-diffusion coefficients have been determined by analyzing the intermediate scattering functions $S(q,t)$ as well as the dynamic structure factor $S(q,\omega)$ (see Refs. [11,38] for details), in order to reduce the impact of systematic errors in the analysis procedure. The mean relaxation time in the energy transfer domain was determined by a numerical Fourier transformation of Eq. (1). The self-diffusion coefficients for $Hf_{35}Ni_{65}$, Hf_{35} $^{60}Ni_{65}$ [11], $Zr_{36}Ni_{64}$ [39], and $Hf_{10}Zr_{25}Ni_{65}$ are shown in Fig. 4(a). The results for $Hf_{10}Zr_{25}Ni_{65}$ are also compiled in Table I.

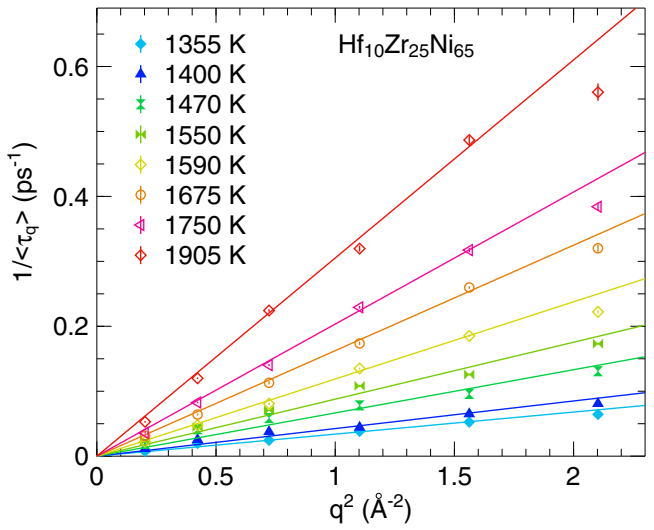

FIG. 3. Inverse structural relaxation time for $Hf_{10}Zr_{25}Ni_{65}$ at 1355, 1400, 1470, 1550, 1590, 1675, 1750, and 1905 K. The linear fit (solid lines) has been performed using (0,0) and values between $q^2 = 0.56$ Å^{-2} and $q^2 = 1.69$ Å^{-2}.

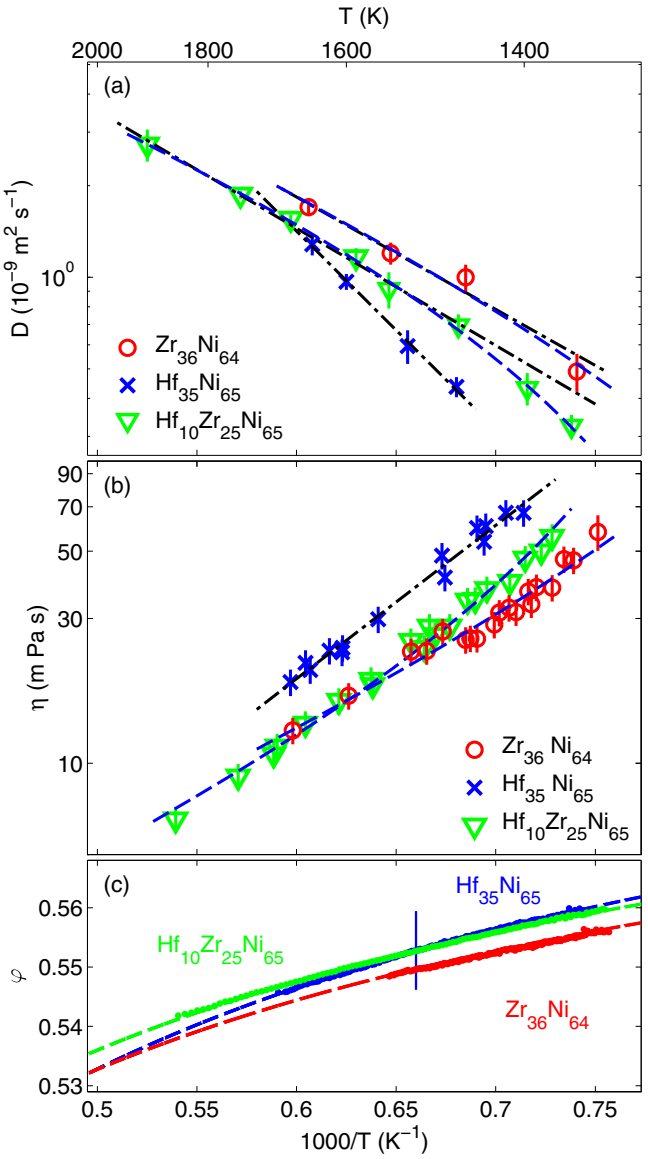

FIG. 4. (a) Self-diffusion coefficients for $Hf_{35}Ni_{65}$ [11], $Zr_{36}Ni_{64}$ [39], and $Hf_{10}Zr_{25}Ni_{65}$ measured by QENS. The black dashed-dotted lines represent the Arrhenius fit and the blue dashed lines the scaling law fit of MCT. (b) Measured viscosity for $Zr_{36}Ni_{64}$ [28], $Hf_{35}Ni_{65}$, and $Hf_{10}Zr_{25}Ni_{65}$ by using the oscillating drop technique in an electrostatic levitator. The black dashed-dotted line represents the Arrhenius fit and the blue lines the scaling law fit of MCT. (c) Packing fraction for $Zr_{36}Ni_{64}$ [40], $Hf_{35}Ni_{65}$ [11], and $Hf_{10}Zr_{25}Ni_{65}$. The blue vertical line reflects the experimental error of the measurement.

The values for the self-diffusion coefficients of $Hf_{10}Zr_{25}Ni_{65}$ are slightly smaller compared to $Zr_{36}Ni_{64}$. Both alloys exhibit an identical activation energy for self-diffusion at higher temperatures ($E_A^{Hf_{10}Zr_{25}Ni_{65}} = (0.76 \pm 0.03)$ eV and $E_A^{Zr_{36}Ni_{64}} = (0.76 \pm 0.11)$ eV), which has been determined by using an Arrhenius fit $D(T) = D_0 \exp[-E_A/(k_B T)]$ [see black dashed-dotted lines in Fig. 4 (a)]. In this formula D_0 is the diffusivity at infinite temperature, k_B the Boltzmann constant, and E_A the activation energy. The calculated diffusivities at infinite temperatures are $D_0^{Zr_{36}Ni_{64}} = (3 \pm 2) \times 10^{-7}$ m^2/s [39] and $D_0^{Hf_{10}Zr_{25}Ni_{65}} = (2.7 \pm 1.3) \times 10^{-7}$ m^2/s. For $Hf_{10}Zr_{25}Ni_{65}$, a deviation from Arrhenius behavior can be observed below ≈1450 K, i.e., about 50 K above the liquidus temperature ($T_L = 1404$ K). Thus, we have only used the measurements above 1450 K for the Arrhenius fit. The atomic dynamics of $Hf_{35}Ni_{65}$, in contrast, are considerably different, as the self-diffusion is lower and the activation energy almost twice as large as for $Hf_{10}Zr_{25}Ni_{65}$ and $Zr_{36}Ni_{64}$ [$E_A^{Hf_{35}Ni_{65}} = (1.31 \pm 0.06)$ eV and $D_0^{Hf_{35}Ni_{65}} = (1.2 \pm 0.2) \times 10^{-5}$ m^2/s]. Around 1680 K the self-diffusion coefficients for $Hf_{10}Zr_{25}Ni_{65}$ and $Hf_{35}Ni_{65}$ are roughly equal.

TABLE I. Measured self-diffusion coefficients for $Hf_{10}Zr_{25}Ni_{65}$.

T (K)	D (10^{-9} m^2 s^{-1})
1355 ± 5	0.33 ± 0.04
1400 ± 5	0.44 ± 0.05
1470 ± 5	0.74 ± 0.09
1550 ± 5	0.97 ± 0.10
1590 ± 5	1.17 ± 0.08
1675 ± 5	1.56 ± 0.05
1750 ± 5	1.87 ± 0.06
1905 ± 5	2.73 ± 0.33

In the entire investigated temperature range the atomic dynamics for $Hf_{10}Zr_{25}Ni_{65}$ are in line with the scaling law of MCT [5]

$$D(T) \propto [(T - T_c)/T_c]^{\gamma}, \quad (2)$$

with a critical temperature $T_c = (1165 \pm 33)$ K and the exponent $\gamma = (1.6 \pm 0.2)$ [see blue dashed line in Fig. 4(a)]. For binary $Zr_{36}Ni_{64}$, the dynamical behavior can be described by the Arrhenius equation (black dashed-dotted line) as well as by the MCT scaling law (blue dashed line) within the experimental errors. In the scaling law fit for $Zr_{36}Ni_{64}$ we used $T_c = 1000$ K from MD simulations [41] as a fixed parameter, since self-diffusion coefficients from QENS measurements and MD simulations are roughly equal [41] and the investigated temperature range of 300 K with only four measured self-diffusion coefficients is too small to perform an adequate fit with T_c and γ as free fit parameters. There is no clear deviation from Arrhenius behavior as for $Hf_{10}Zr_{25}Ni_{65}$, not even at the liquidus temperature. This might be explained by the fact that the Arrhenius equation is an approximation of the MCT scaling law at high temperatures ($T \gg T_c$) [5]. Since the investigated temperature range for $Hf_{35}Ni_{65}$ of 175 K is even smaller compared to $Zr_{36}Ni_{64}$ and we are also not aware of a literature value for T_c, we have only performed an Arrhenius fit for this alloy, which describes accurately the measured self-diffusion coefficients (black dashed-dotted line).

In order to study the effect of partial substitution of Zr by Hf and, thus, of different atomic interactions not only on the microscopic but also on the collective dynamics, the measured viscosities for $Zr_{36}Ni_{64}$ [28], $Hf_{35}Ni_{65}$, and $Hf_{10}Zr_{25}Ni_{65}$ are shown in Fig. 4(b). Towards lower temperatures the viscosity at constant temperature seems to increase with an increasing Hf concentration. While the viscosity of $Hf_{10}Zr_{25}Ni_{65}$ below 1500 K is slightly higher compared to $Zr_{36}Ni_{64}$, the viscosities

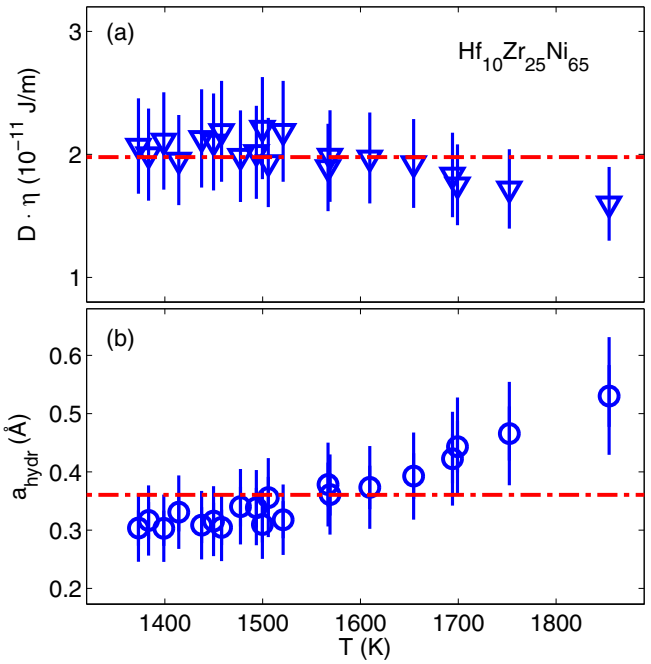

FIG. 5. (a) $D \cdot \eta$ for $Hf_{10}Zr_{25}Ni_{65}$ as a function of temperature. The red dashed-dotted line is the calculated mean value. (b) Hydrodynamic radius a_{hydr} derived from the Stokes-Einstein relation. The red dashed-dotted line is the mean value.

of the two compositions are roughly equal at higher temperatures. The melt viscosities of $Hf_{35}Ni_{65}$ follow an Arrhenius behavior with a calculated activation energy of $E_A = (1.00 \pm 0.04)$ eV [black dashed-dotted line in Fig. 4(b)]. The collective dynamics for $Zr_{36}Ni_{64}$ can be described by the MCT scaling law [blue dashed line in panel (b)] similar to the self-diffusion, albeit with a negative value of γ. The critical temperature has been fixed to $T_c = 1000$ K in the fitting procedure as well, due to the small investigated temperature range and the larger experimental error compared to measured self-diffusion coefficients. The calculated exponent $\gamma_\eta = 1.95 \pm 0.10$ is nearly equal in comparison to self-diffusion ($\gamma_D = 1.97 \pm 0.22$). The measured viscosities for $Hf_{10}Zr_{25}Ni_{65}$ follow a MCT scaling law similar to the self-diffusion coefficients (blue dashed line). The fit of measured viscosities using the critical temperature from self-diffusion ($T_c = 1165$ K) as a fixed parameter yields a roughly equal exponent for the viscosity ($\gamma_\eta = 1.77 \pm 0.03$) compared to the self-diffusion ($\gamma_D = 1.6 \pm 0.2$).

The packing fractions in Fig. 4(c), which have been derived from macroscopic density measurements, are nearly identical at same temperatures for binary/ternary Hf-/Zr-Ni melts. The systematic error of the calculated packing fractions between different measurements of ≈1% (indicated as the blue vertical line) can be derived from the experimental error of the density measurements due to the limited camera resolution. The relative error of the measured density in a single measurement, however, is much smaller compared to the systematic error (see Ref. [42] for details).

As raised in the introduction, the investigation of the connection between self-diffusion and viscosity is of essential interest concerning predictions of MCT. For this purpose, the product $D \cdot \eta$ has been calculated and is shown in Fig. 5(a) as a function of temperature.

For determing $D \cdot \eta$, the measured viscosity at a given temperature [see Fig. 4(b)] was multiplied with the power law fit of $D^{Hf_{10}Zr_{25}Ni_{65}}$ [blue dashed line in panel (a)], as the error of the measured self-diffusion coefficients is smaller compared to that of the measured viscosities. The mean value is $\overline{D \cdot \eta} = (1.98 \pm 0.16) \times 10^{-11}$ J/m over the temperature range from 1383 to 1854 K [red dashed-dotted line in Fig. 5(a)]. In order to investigate the nonvalidity of the SE relation, the hydrodynamic radius a_{hydr}, which has been calculated by using the SE relation [18], is shown in Fig. 5(b).

IV. DISCUSSION

The substitution of Zr by Hf, which have nearly identical atomic sizes but have been shown to exhibit different chemical interactions with the smaller Ni atoms, leads to a reduced self-diffusion and a higher viscosity of the melt, which cannot be explained by packing fraction arguments, as the measured packing fraction remains nearly identical at the same temperatures over the investigated temperature range within the experimental uncertainties for the binary and ternary melts [see Fig. 4(c)]. Thus, the different dynamical behavior might be explained by an increased number of Hf-Ni and a reduced number of Zr-Ni interactions, highlighting the important role of the CSRO in these binary and ternary glass-forming metallic melts.

Due to the large temperature range over which the self-diffusion coefficients for $Hf_{10}Zr_{25}Ni_{65}$ were measured, we can identify a distinct deviation from Arrhenius behavior above the liquidus temperature. The liquidus temperature of $Hf_{10}Zr_{25}Ni_{65}$ ($T_L = 1404$ K) lies in between that of $Zr_{36}Ni_{64}$ ($T_L = 1343$ K) and $Hf_{35}Ni_{65}$ ($T_L = 1463$ K), but in contrast to the ternary melt, the binary systems can be well described by the Arrhenius equation even around the liquidus temperature. In the binary $Zr_{64}Ni_{36}$ melt a deviation has been observed more than 100 K below T_L [40], while for multicomponent bulk metallic glass formers, such as Vit1, Vit4, and Pd-Cu-Ni-P, a deviation from Arrhenius behavior has been identified above the melting point [5,31], similar to $Hf_{10}Zr_{25}Ni_{65}$. Hence, an increased number of atomic components in the melt seems to result in a higher critical temperature, which leads to a deviation from Arrhenius behavior even above the melting point, where the measured self-diffusion coefficients are instead well described by the MCT scaling law. For $Hf_{10}Zr_{25}Ni_{65}$ and $Zr_{36}Ni_{64}$, not only the self-diffusion but also the measured viscosity is in line with the MCT scaling law, using identical critical temperatures and similar exponents γ for the corresponding melt. The substitution of Zr by Hf results in a higher T_c for $Hf_{10}Zr_{25}Ni_{65}$ ($T_c^{Hf_{10}Zr_{25}Ni_{65}} = 1165$ K) in comparison to $Zr_{36}Ni_{64}$, for which MD simulations predict a critical temperature of about $T_c^{Zr_{36}Ni_{64}} = 1000$ K [41]. We can therefore conclude that the substitution of only 10 at.% Zr by Hf leads to an increased T_c of about 165 K and consequently to a decreased difference $\Delta T_{LC} = T_L - T_c$ from $\Delta T_{LC}^{Zr_{36}Ni_{64}} = 343$ K to $\Delta T_{LC}^{Hf_{10}Zr_{25}Ni_{65}} = 239$ K. Keeping in mind that a higher reduced glass transition temperature $T_{rg} = T_g/T_L$ has been positively correlated to the GFA [43–45], we have calculated

a reduced critical temperature $T_{rc} = T_c/T_L$ while assuming, in a first approximation, a linear relation between T_c and T_g. Following this, as a result of the substitution of Zr by Hf, T_{rc} increases from $T_{rc}^{Zr_{36}Ni_{64}} = 0.75$ to $T_{rc}^{Hf_{10}Zr_{25}Ni_{65}} = 0.83$. The smaller $\Delta T_{LC}^{Hf_{10}Zr_{25}Ni_{65}}$ and larger $T_{rc}^{Hf_{10}Zr_{25}Ni_{65}}$ can thus be correlated to slower atomic dynamics in $Hf_{10}Zr_{25}Ni_{65}$ at lower temperatures compared to $Zr_{36}Ni_{64}$. The difference between the corresponding self-diffusion coefficients of the two alloys at a fixed temperature increases towards lower temperatures [see Fig. 4(a)]. The same conclusion can be drawn from the measured melt viscosity in Fig. 4(b), which increases faster with decreasing temperature for the ternary melt. This might underline the statement raised in the introduction, that an increased number of atomic components in $Hf_{10}Zr_{25}Ni_{65}$ seems to enhance the GFA in comparison to $Zr_{36}Ni_{64}$ due to slower atomic and collective dynamics towards lower temperatures. In the past lower diffusivities have been related to the good GFA found in, e.g., some Zr-Cu compositions [46]. Further approaches to classify glass-forming liquids use the enthalpy of mixing or the number of various elements with different atomic sizes in the melt [47–49]. For $Hf_{10}Zr_{25}Ni_{65}$, however, the sluggish dynamics are not caused by increased atomic size differences, since for covalent radii $r_{cov}^{Hf} \approx r_{cov}^{Zr}$ [12] applies and for Goldschmidt radii $r_G^{Hf} \approx r_G^{Zr}$ [50], but because of an increased number of different chemical interactions. The important role of chemical interactions in metallic melts and the impact on dynamical and structural features has been recently studied in terms of the addition of Al to Zr-Ni/Co/Cu melts [10,51,52]. However, in contrast to binary/ternary Hf-/Zr-Ni alloys, the packing fraction is not constant upon the addition of Al, which thus prevents a conclusive explanation.

To study the impact of component addition also on the connection between different dynamical properties, in this case the relation between microscopic and macroscopic dynamics, we have calculated the product of self-diffusion and viscosity $D \cdot \eta$ [see Fig. 5(a)]. Since both can be described by the MCT scaling law using almost equal parameters, the product $D \cdot \eta$ is therefore roughly constant. This is consistent with predictions from MCT, which implies an identical critical exponent γ in the scaling law $[(T - T_c)/T_c]^{\gamma}$ for the behavior of D and η^{-1} when approaching T_c [17]. For $Hf_{10}Zr_{25}Ni_{65}$, both the self-diffusion and the viscosity can be described in the framework of MCT even at high temperatures up to ≈1700 K. Towards even higher temperatures, however, the data point at 1854 K is slightly smaller than the mean value of $\overline{D \cdot \eta} = (1.98 \pm 0.16) \times 10^{-11}$ J/m [red dashed-dotted line in Fig. 5(a)]. This might be explained by both the larger error of the MCT predictions for $T \gg T_c$ and data uncertainties in the viscosity measurements at high temperatures due to the low viscosity ($\eta < 10$ mPa s for $T > 1700$ K). Furthermore, the nearly constant product $D \cdot \eta$ might indicate a nonvalidity of the Stokes-Einstein (SE) relation [18]. For this purpose, we have calculated the effective hydrodynamic radius yielding a mean value of $\overline{a}_{hydr} = (0.36 \pm 0.06)$ Å, which is indeed too small for an atomic radius in a dense metallic liquid. In addition to this, the almost doubling of a_{hydr} in a temperature range of approximately 500 K is physically not reasonable [see Fig. 5(b)], lending more experimental evidence to our findings that the SE relation is not valid in $Hf_{10}Zr_{25}Ni_{65}$. This conclusion is independent of whether slip or stick conditions are used in the SE relation [53]. As the experimental effort to perform viscosity and self-diffusion measurements for metallic liquids in an adequate temperature range with a sufficiently small experimental error is very large, the nonvalidity of the SE relation has been only demonstrated so far experimentally for the binary metallic melt $Zr_{64}Ni_{36}$ [19] and for $Zr_{46.5}Ti_{18.2}Cu_{7.5}Ni_{10}Be_{27.5}$ [20]. Recently, MD simulations have demonstrated a breakdown of the SE relation for liquid Al-Cr [6] and Cu-Zr-Al [54] at a respective specific temperature where this breakdown was associated with a change from an Arrhenius to a non-Arrhenius behavior. While for these alloys the breakdown of the SE relation has been related to dynamical heterogeneities, other studies, in contrast, seem to imply that there is no connection at all [55,56]. For $Hf_{10}Zr_{25}Ni_{65}$ a nonvalidity of the SE relation has been observed over the entire temperature range, but a change from an Arrhenius to a non-Arrhenius behavior around 1450 K. This finding underlines the fact that there is no profound understanding of this connection for metallic melts in general, since a distinct structural origin has yet to be identified.

Concerning the comparison between these ternary and binary systems, we will now discuss the origin of the significantly different dynamical behavior of $Hf_{35}Ni_{65}$ compared to $Hf_{10}Zr_{25}Ni_{65}$ and $Zr_{36}Ni_{64}$. Recently, the larger activation energy for $Hf_{35}Ni_{65}$ compared to $Zr_{36}Ni_{64}$ has been explained by a smaller interatomic distance between Hf-Hf nearest-neighbor pairs in $Hf_{35}Ni_{65}$ in comparison to Zr-Zr nearest-neighbor pairs in $Zr_{36}Ni_{64}$. This has been interpreted as a locally higher packing density of Hf atoms in $Hf_{35}Ni_{65}$ [11]. Since the activation energy for $Hf_{10}Zr_{25}Ni_{65}$ determined by using the self-diffusion coefficients at $T > 1450$ K is equal to $Zr_{36}Ni_{64}$ and not as large as for $Hf_{35}Ni_{65}$, it is reasonable to conclude that the fraction of Hf-Hf nearest-neighbor pairs in the ternary melt is too small to raise the activation energy. The atomic dynamics are thus similar to $Zr_{36}Ni_{64}$ and show larger differences in comparison to $Hf_{35}Ni_{65}$. As a consequence, our findings are in line with our previous explanation concerning the different dynamical behavior due to the distinct structural differences between $Zr_{36}Ni_{64}$ and $Hf_{35}Ni_{65}$ [11].

In these two binary metallic melts dynamically decoupled self-diffusion coefficients have been recently identified, i.e., the self-diffusion of larger Zr and Hf atoms is reduced in comparison to the smaller Ni atoms. Although we were only able to obtain information on the Ni-dominated self-diffusion in $Hf_{10}Zr_{25}Ni_{65}$ (≈93%), the observed average stretching exponent $\overline{\beta} = 0.85$ implies heterogenous atomic dynamics. The stretching of the exponential function can be explained by the presence of different relaxation times due to faster and slower atoms in the melt, which leads to a superposition of faster and slower exponential decays in the intermediate scattering function $S(q,t)$. For $Zr_{36}Ni_{64}$ and $Hf_{35}Ni_{65}$, in contrast, the measured $S(q,t)$ can be described by a simple exponential decay ($\beta = 1$). Based on the pronounced stretching behavior of the measured $S(q,t)$ for $Hf_{10}Zr_{25}Ni_{65}$ ($\overline{\beta} = 0.85$), one thus might conclude that the factor of decoupling in the ternary melt is larger compared to the recently identified factor of decoupling in $Zr_{36}Ni_{64}$ ($D_{Ni}/D_{Zr} \approx 1.8$) [16] and $Hf_{35}Ni_{65}$ ($D_{Ni}/D_{Hf} \approx 2$) [11].

V. SUMMARY

The glass-formation process is controlled by many different physical properties such as atomic size differences, packing fractions, and competing chemical interactions. In order to investigate the impact of these features on the dynamical behavior, which in turn governs the glass-formation process, we studied the ternary melt $Hf_{10}Zr_{25}Ni_{65}$ through detailed measurements of self-diffusion coefficients and viscosity.

Our results demonstrate that the measured self-diffusion coefficients and the viscosities for $Hf_{10}Zr_{25}Ni_{65}$ can be accurately described through the MCT scaling law. Our analysis reveals a higher critical temperature T_c for the ternary melt compared to the binary alloy $Zr_{36}Ni_{64}$, even though we substitute only small amounts of similar sized atomic components at nearly constant measured packing fractions. Thus, we are able to disentangle the influence of packing fraction and that of chemical interactions on the dynamical behavior, which is important because the effect of geometric packing induced by mixing different sizes of atoms is also not trivial. In contrast to $Zr_{36}Ni_{64}$, we observed a distinct deviation from Arrhenius behavior for $Hf_{10}Zr_{25}Ni_{65}$ already below 1450 K. Hence, the atomic and collective dynamics in $Hf_{10}Zr_{25}Ni_{65}$ are slower compared to binary $Zr_{36}Ni_{64}$, in particular at lower temperatures. This may imply a higher GFA for the ternary melt, which might be correlated to the smaller difference $\Delta T_{LC} = T_L - T_c$ or the larger reduced critical temperature $T_{rc} = T_c/T_L$ in comparison to $Zr_{36}Ni_{64}$.

One of the most important features is the stretched exponential behavior of the measured $S(q,t)$ for $Hf_{10}Zr_{25}Ni_{65}$, which might imply an enlarged factor of decoupling in the ternary melt compared to the binary systems $Zr_{36}Ni_{64}$ and $Hf_{35}Ni_{65}$. This finding highlights that the dynamical behavior for $Hf_{10}Zr_{25}Ni_{65}$ is not simply a superposition of the dynamics of the two binary parent alloys, but depends on the different (additional) atomic interactions, since the activation energy of the self-diffusion is very similar to that of $Zr_{36}Ni_{64}$, but the absolute value of self-diffusion for $Hf_{10}Zr_{25}Ni_{65}$ is smaller compared to $Zr_{36}Ni_{64}$. In addition, the measured melt viscosities show a similar behavior as the self-diffusion, since the viscosities for $Hf_{10}Zr_{25}Ni_{65}$ exhibit a stronger increase at lower temperatures in comparison to the binary melts, which leads to the conclusion that there is also no superposition of the viscosities of the binary parent alloys. The observed differences cannot be explained by packing arguments, since the measured packing fraction for binary and ternary Hf-/Zr-Ni melts is nearly identical.

The origin for the overall more sluggish dynamics with an increased amount of Hf might thus be mainly attributed to the different chemical interactions in the melts, i.e., an increased number of Hf-Ni and a reduced number of Zr-Ni interactions. Moreover, additional Zr-Hf interactions in $Hf_{10}Zr_{25}Ni_{65}$ may also influence the dynamical behavior even though the fraction of Zr-Hf nearest-neighbor pairs should be very small due to the low Zr and Hf concentrations. Since it is not possible to experimentally determine partial structure factors for the ternary alloy melt, additional MD simulations might help analyzing structural influences on the dynamics.

As a general result, the self-diffusion coefficients are reduced and viscosities increase as a function of increasing Hf content of the melt. The atomic dynamics for $Hf_{10}Zr_{25}Ni_{65}$ are significantly different in comparison to $Hf_{35}Ni_{65}$, which exhibits an activation energy of self-diffusion that is nearly twice as large as for $Zr_{36}Ni_{64}$ and $Hf_{10}Zr_{25}Ni_{65}$. As indicated in Ref. [11] this can be explained by a smaller interatomic distance between Hf-Hf compared to Zr-Zr. The amount of Hf atoms in the ternary melt, however, seems to be too low to raise the activation energy of self-diffusion as for $Hf_{35}Ni_{65}$. Further experimental studies are required in order to elucidate composition dependence over a broader compositional range.

ACKNOWLEDGMENTS

We would like to thank Sarah Zimmermann, Patrick Fopp, and Sandro Szabó for their help during the experiments at FRM-II and Eugen Ritter for his help during the viscosity measurements. Wiebke Lohstroh and Herbert Meier are gratefully acknowledged for their technical support at the TOFTOF spectrometer. We gratefully acknowledge support from the German Research Foundation (DFG) via Grant No. EV211/2-1.

[1] A. Greer and E. Ma, MRS Bull. **32**, 611 (2007).
[2] H. Tanaka, J. Non-Cryst. Solids **351**, 678 (2005).
[3] O. N. Senkov, Phys. Rev. B **76**, 104202 (2007).
[4] M. Ediger and P. Harrowell, J. Chem. Phys. **137**, 080901 (2012).
[5] A. Meyer, Phys. Rev. B **66**, 134205 (2002).
[6] N. Jakse and A. Pasturel, Phys. Rev. B **95**, 144210 (2017).
[7] N. Jakse and A. Pasturel, Phys. Rev. B **78**, 214204 (2008).
[8] F. Yang, D. Holland-Moritz, J. Gegner, P. Heintzmann, F. Kargl, C. C. Yuan, G. G. Simeoni, and A. Meyer, Europhys. Lett. **107**, 46001 (2014).
[9] S. M. Chathoth, B. Damaschke, M. M. Koza, and K. Samwer, Phys. Rev. Lett. **101**, 037801 (2008).
[10] C. C. Yuan, F. Yang, F. Kargl, D. Holland-Moritz, G. G. Simeoni, and A. Meyer, Phys. Rev. B **91**, 214203 (2015).
[11] B. Nowak, D. Holland-Moritz, F. Yang, T. Voigtmann, Z. Evenson, T. C. Hansen, and A. Meyer, Phys. Rev. B **96**, 054201 (2017).
[12] L. Pauling, J. Am. Chem. Soci. **69**, 542 (1947).
[13] L. Shadowspeaker and R. Busch, Appl. Phys. Lett. **85**, 2508 (2004).
[14] S. W. Basuki, A. Bartsch, F. Yang, K. Rätzke, A. Meyer, and F. Faupel, Phys. Rev. Lett. **113**, 165901 (2014).
[15] S. W. Basuki, F. Yang, E. Gill, K. Rätzke, A. Meyer, and F. Faupel, Phys. Rev. B **95**, 024301 (2017).
[16] B. Nowak, D. Holland-Moritz, F. Yang, T. Voigtmann, T. Kordel, T. Hansen, and A. Meyer, Phys. Rev. Materials **1**, 025603 (2017).
[17] W. Götze, *Complex Dynamics of Glass-Forming Liquids: A Mode-Coupling Theory*, Vol. 143 (Oxford University Press, Oxford, New York, 2009).
[18] A. Einstein, Ann. Phys. **322**, 549 (1905).
[19] J. Brillo, A. I. Pommrich, and A. Meyer, Phys. Rev. Lett. **107**, 165902 (2011).
[20] F. Yang, T. Unruh, and A. Meyer, Europhys. Lett. **107**, 26001 (2014).

[21] T. Unruh, J. Neuhaus, and W. Petry, Nucl. Instrum. Methods Phys. Res., Sect. A **580**, 1414 (2007).
[22] W. Lohstroh and Z. Evenson, J. Large-Scale Res. Facil. **1**, 1 (2015).
[23] V. F. Sears, Neutron News **3**, 26 (1992).
[24] T. Kordel, D. Holland-Moritz, F. Yang, J. Peters, T. Unruh, T. Hansen, and A. Meyer, Phys. Rev. B **83**, 104205 (2011).
[25] D. Holland-Moritz, T. Schenk, P. Convert, T. Hansen, and D. M. Herlach, Meas. Sci. Technol. **16**, 372 (2005).
[26] D. Holland-Moritz, S. Stüber, H. Hartmann, T. Unruh, T. Hansen, and A. Meyer, Phys. Rev. B **79**, 064204 (2009).
[27] F. Yang, T. Kordel, D. Holland-Moritz, T. Unruh, and A. Meyer, J. Phys. Condens. Matter **23**, 254207 (2011).
[28] P. Heintzmann, F. Yang, S. Schneider, G. Lohöfer, and A. Meyer, Appl. Phys. Lett. **108**, 241908 (2016).
[29] J. Brillo and I. Egry, Int. J. Thermophys. **24**, 1155 (2003).
[30] C. A. Angell, K. L. Ngai, G. B. McKenna, P. F. McMillan, and S. W. Martin, J. Appl. Phys. **88**, 3113 (2000).
[31] A. Meyer, W. Petry, M. Koza, and M.-P. Macht, Appl. Phys. Lett. **83**, 3894 (2003).
[32] S. M. Chathoth, A. Meyer, M. Koza, and F. Juranyi, Appl. Phys. Lett. **85**, 4881 (2004).
[33] Z. Evenson, F. Yang, G. G. Simeoni, and A. Meyer, Appl. Phys. Lett. **108**, 121902 (2016).
[34] R. Kohlrausch, Ann. Phys. **167**, 179 (1854).
[35] G. Williams and D. C. Watts, Trans. Faraday Soc. **66**, 80 (1970).
[36] A. Meyer, R. Busch, and H. Schober, Phys. Rev. Lett. **83**, 5027 (1999).
[37] J. P. Boon and S. Yip, *Molecular hydrodynamics* (McGraw-Hill, New York, 1980).
[38] J. Hansen and I. McDonald, *Theory of Simple Liquids* (Academic Press Limited, London, 1986).
[39] D. Holland-Moritz, S. Stüber, H. Hartmann, T. Unruh, and A. Meyer, J. Phys. Conf. Ser. **144**, 012119 (2009).
[40] T. Kordel Nahordnung und atomare Dynamik in elektrostatisch levitierten Zr-Basis-Schmelzen, Ph.D. thesis, school Ruhr-Universität Bochum 2011.
[41] P. Kuhn, J. Horbach, F. Kargl, A. Meyer, and T. Voigtmann, Phys. Rev. B **90**, 024309 (2014).
[42] H. Yoo, C. Park, S. Jeon, S. Lee, and G. W. Lee, Metrologia **52**, 677 (2015).
[43] D. Turnbull, Contemp. Phys. **10**, 473 (1969).
[44] A. Drehman and A. Greer, Acta Metall. **32**, 323 (1984).
[45] A. Peker and W. L. Johnson, Appl. Phys. Lett. **63**, 2342 (1993).
[46] S. Hao, C. Wang, M. Kramer, and K. Ho, J. Appl. Phys. **107**, 053511 (2010).
[47] A. Inoue and A. Takeuchi, Mater. Trans. **43**, 1892 (2002).
[48] A. Takeuchi and A. Inoue, Mater. Trans. **46**, 2817 (2005).
[49] J. Basu, B. Murty, and S. Ranganathan, J. Alloys Compd. **465**, 163 (2008).
[50] C. J. Smithells, *Smithells Metals Reference Book*, edited by E. A. Brandes (Butterworths & co., London, 1983).
[51] Y. Q. Cheng, E. Ma, and H. W. Sheng, Phys. Rev. Lett. **102**, 245501 (2009).
[52] X. Xi, M. Sandor, H. Wang, J. Wang, W. Wang, and Y. Wu, J. Phys. Condens. Matter **23**, 115501 (2011).
[53] F. Affouard, M. Descamps, L.-C. Valdes, J. Habasaki, P. Bordat, and K. L. Ngai, J. Chem. Phys. **131**, 104510 (2009).
[54] A. Jaiswal, T. Egami, and Y. Zhang, Phys. Rev. B **91**, 134204 (2015).
[55] S. R. Becker, P. H. Poole, and F. W. Starr, Phys. Rev. Lett. **97**, 055901 (2006).
[56] H. C. Andersen, Proc. Natl. Acad. Sci. USA **102**, 6686 (2005).